Journal of Hazardous Materials 344 (2018) 1034–1042

Contents lists available at ScienceDirect

Journal of Hazardous Materials

journal homepage: www.elsevier.com/locate/jhazmat

Fast adsorption of heavy metal ions by waste cotton fabrics based double network hydrogel and influencing factors insight

Jianhong Ma[a,b], Yutang Liu[a,b,*], Omar Ali[a,b], Yuanfeng Wei[c], Shuqu Zhang[c], Yuanmeng Zhang[c], Tao Cai[a,b], Chengbin Liu[c], Shenglian Luo[c]

[a] College of Environmental Science and Engineering, Hunan University,Lushan South Road, Yuelu District, Changsha 410082, PR China
[b] Key Laboratory of Environmental Biology and Pollution Control (Hunan University), Ministry of Education,Lushan South Road, Yuelu District, Changsha 410082, PR China
[c] State Key Laboratory of Chemo/Biosensing and Chemometrics, Hunan University,Lushan South Road, Yuelu District, Changsha 410082, PR China

HIGHLIGHTS

- Recycling of waste cotton fabrics as an efficient heavy metal adsorbent;.
- Fast adsorption kinetics of achieving adsorption equilibrium in five minutes;.
- Fix-bed columns can efficiently remove heavy metal ions in simulated influent;.
- The material can effectively handle the practical industrial effluent.

GRAPHICAL ABSTRACT

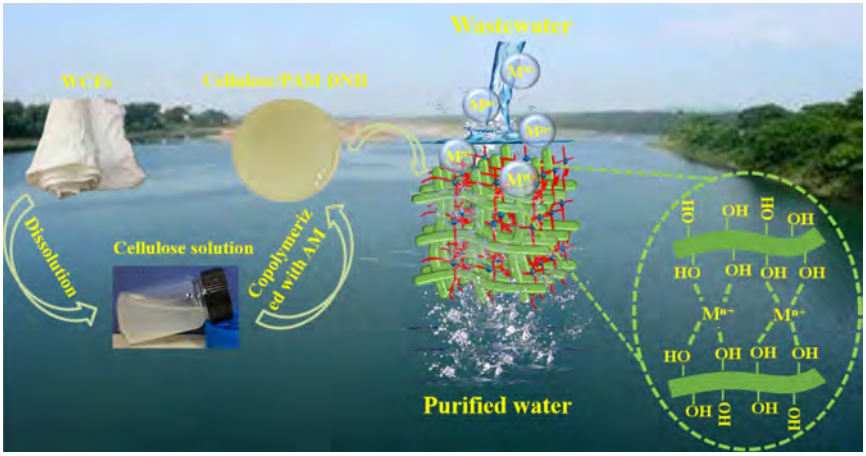

ARTICLE INFO

Article history:
Received 28 July 2017
Received in revised form
22 November 2017
Accepted 23 November 2017
Available online 1 December 2017

Keywords:
Waste cotton fabrics
Hydrogel
Heavy metal adsorption
Fixed-bed column
Industrial effluent

ABSTRACT

Massive consumption of cotton fabrics has brought up a serious problem concerning the waste cotton fabrics (WCFs) disposal. It is widely accepted that if WCFs can be reutilized, there will be great business potentials. Herein, we prepared a double network hydrogel based on WCFs and polyacrylamide (Cellulose/PAM DNHs) for heavy metal removal. The DNHs exhibit fast kinetics that sorption equilibrium is achieved in 5 min because of the porous and sheet-like laminar structures they possess. The DNHs also illustrate excellent adsorption property and good reusability. The tandem two columns packed with Cellulose/PAM-3 can effectively process simulated and practical wastewater, and the adsorption discrepancy is negligible after three adsorption-desorption cycles. The treatment volumes of simulated wastewater are 172.5 BV (7935 mL), 195 BV (8970 mL), and 292.5 BV (13455 mL) for Cd(II), Cu(II), and Pb(II), respectively. Furthermore, the treatment volumes of practical industrial wastewater reach 42 BV (1932 mL) for Cd(II), 63 BV (2898 mL) for Cu(II), and 87 BV (4002 mL) for Zn(II), Pb(II) and Fe, respectively. This work provides a new avenue for the combination of WCFs reuse and heavy metal removal, which is of great importance to the construction of resource sustainability and environment-friendly society.

* Corresponding author at: College of Environmental Science and Engineering, Hunan University, Lushan South Road, Yuelu District, Changsha 410082, P.R. China.
E-mail addresses: yt_liu@hnu.edu.cn, liuyutang@126.com (Y. Liu).

https://doi.org/10.1016/j.jhazmat.2017.11.041
0304-3894/

1. Introduction

Heavy metal pollution in waters is a worldwide and serious environmental issue due to their toxicity and carcinogenicity [1]. Especially, toxic heavy metal ions, like Cd(II), Cu(II) and Pb(II), have attracted the most attention and become a research focus [2–4]. Various techniques have been employed for heavy metal removal, such as chemical precipitation, membrane, adsorption, and electrodialysis [5]. Among these available techniques, adsorption has been viewed as one of the most attractive options for its easy operation and high cost effectiveness [6]. Therefore, to further improve the cost effectiveness of adsorption process, there is a growing need to develop low-cost, renewable, locally available materials as adsorbent. Notably, waste materials and by-products from agriculture and industry have been widely used for wastewater treatment, such as biogas residues [7], chitosan [8], saccharomyces cerevisiae [9] and biomass [10]. Most of them belong to nanomaterials which possess large surface areas, easy modification, and large number of active sites in favor of heavy metal removal. However, these materials still suffer from drawbacks such as complex preparation process, as well as difficulty in separation and regeneration.

Vast waste cotton fabrics (WCFs) are generated as the steady increase of cotton textile consumption in the past few decades. Additionally, the disposing methods of WCFs, specifically landfill and incineration, will not only create environmental pollution, but also lead to great waste of valuable resources [11]. Significant progress has been achieved over the past decade in recycling WCFs, including applied to pollutants removal [12,13], cellulose nanocrystals extraction [14], sodium-ion batteries [15], cloth actuator [16] and thermal insulating materials [17] preparation. Little is known, however, about possible applications for heavy metal removal. In general, the WCFs can dissolute in NaOH/urea aqueous solution, forming viscosity cellulose solution and exposing the reactive functional groups [18]. Cellulose, formed by the repeated connection of D-glucose building blocks, possessing characteristics of hydrophilicity, chirality, biodegradability, broad chemical modification capacity, and ability to form versatile semicrystalline fiber morphologies [19].

Recently, double network hydrogel (DNH), comprising two interpenetrating and cross-linked polymer networks, has stimulated research enthusiasm, because of its adjustable performance [20–22]. The DNH significantly improves hydrogel mechanical properties, and it can be produced and optimized in a fast and controllable manner using one-pot strategy [23]. The high-water content of DNH facilitates water permeability and the entry of foreign ions into DNH interior [24]. Thus, if some functional groups are introduced into the DNH structure, all will be excellent adsorbent.

Herein, taking cotton scraps collected from dyeing factory as an example of WCFs, we prepared viscosity cellulose solution using NaOH/urea aqueous solution. Then, DNHs based on cellulose and polyacrylamide (Cellulose/PAM DNHs) were prepared by one-pot strategy. The main objective of this study is to reveal the underpinned relation between the amount of crosslinking agent and adsorption performance of the obtained materials, which is particularly important for the practical application of Cellulose/PAM DNHs. To this end, the sorption performance and mechanism of heavy metals onto Cellulose/PAM DNHs are revealed by a series structural characterization and batch sorption runs. On the basis of gathered experimental data, it inferred that the adsorption performance is highly related to the crosslinking density of cellulose network. More importantly, for the first time, a novel WCFs based DNH was prepared and applied in heavy metal removal, which can provide inspiration for future studies in WCFs disposal and heavy metal removal.

2. Materials and methods

2.1. Chemicals and materials

Waste cotton fabrics (WCFs) without further purification or bleaching were collected from dyeing and weaving factory. Urea and acrylamide (AM, AR) were purchased from Sinopharm Chemical Reagent Co., Ltd. Potassium persulfate (KPS, AR) and N, N-methylenebisacrylamide (MBA, AR) were provided by Shanghai Xitang Biotechnology Co., Ltd., China. Epichlorohydrin (ECH, AR) was purchased from Aladdin Chemistry Co, Ltd. All the chemicals were used as received without further purification. All aqueous solutions were prepared with deionized water.

2.2. Preparation of Cellulose/PAM DNHs

Initially, WCFs were smashed into pieces, and dissolved in NaOH-based aqueous system by two-step process. 4 g WCFs was dispersed in 48 g 14 wt% NaOH aqueous solution pre-cooled to 0 °C and stirred for 1 min. Then, 48 g 24 wt% urea aqueous solution pre-cooled to 0 °C was added immediately with stirring vigorously for 2 min, resulting a viscous cellulose solution. Then, 6 mL cellulose solution was added to the aqueous contains 1.0 g AM, 0.6 mol% KPS (initiator for AM), 2 mol% MBA (crosslinker) and 2 mL deionized water. Afterwards, different amounts of ECH (0, 0.2, 0.3, 0.4, 0.5, 0.6 mL) were added to the mixed solution to form different materials, and the samples were named Cellulose/PAM-1, Cellulose/PAM-2, Cellulose/PAM-3, Cellulose/PAM-4, Cellulose/PAM-5, and Cellulose/PAM-6. The obtained sol was bubbled and injected into box of silica gel ice cubes (1 cm × 1 cm × 1 cm) and the box was presented in a forced convection oven for 2 h at 60 °C to complete the gelation process. The synthetic cost of dried Cellulose/PAM DNHs is approximately US$ 8.7×10^3/t (see in Supporting Information, SI). The overall preparation process of Cellulose/PAM DNHs is shown in Fig. 1.

2.3. Characterizations

The surface morphologies of these samples were examined by field emission scanning electron microscopy (SEM, Hitachi S-4800). Swelling ratio of the DNHs was calculated as $SR = (W_s - W_d)/W_d$, moisture content of the swollen samples was calculated as $(W_s - W_d)/W_s \times 100\%$, where W_s and W_d are the weight of swollen and dried samples, respectively. Compression tests were performed on a MTS 858 Bionix Test System (MTS System Co., Minneapolis, MN). The thermogravimetric analysis (TGA) was measured under a nitrogen atmosphere with a TG/DTA7300 from room temperature to 700 °C with heating rate of 10 °C/min. The functional groups of samples were detected using a Fourier transform infrared Nicolet 5700 spectrophotometer (FTIR, American). The crystal phases of the samples were analyzed by an X-ray diffractometer with Cu-Kα radiation (XRD, M21X, MAC Science Ltd., Japan). ^{13}C CP/MAS NMR experiments were performed on Bruker AVANCE III 600 spectrometer at a resonance frequency of 150.9 MHz. The chemical shifts of ^{13}C was externally referenced to TMS. UV–vis diffuse reflectance spectra (DRS) were recorded on a UV–vis spectrophotometer (Cary 300, USA) with an integrating sphere. The pH value at the point of zero charge (pH_{PZC}) of the DNHs was measured by ΔpH drift method in a series of 0.01 M NaCl aqueous with different initial pH. The surface chemistry of the adsorbent was determined by X-ray photoelectron spectroscopy (XPS, K-Alpha 1063, Thermo Fisher Scientific, England).

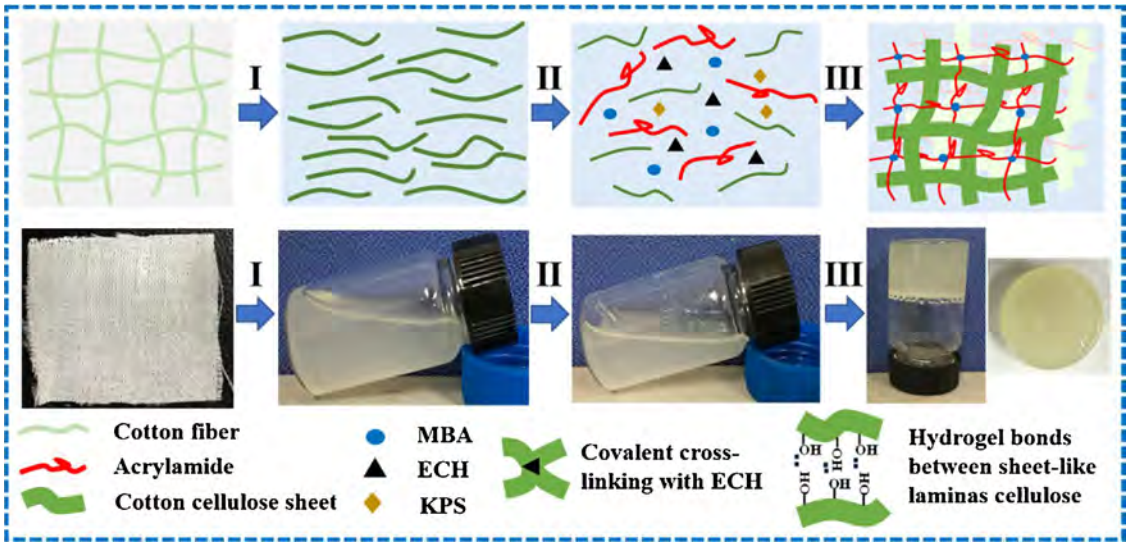

Fig. 1. Preparation of Cellulose/PAM DNHs. (I) Dissolution of WCFs, (II) preparation of sol containing cellulose solution, AM, MBA, KPS, and ECH, (III) the gelation of the obtained sol.

2.4. Batch sorption of heavy metals

Analytical grade heavy metal nitrate salts ($Cu(NO_3)_2$, $Cd(NO_3)_2$ and $Pb(NO_3)_2$) were employed to prepare the stock solutions. The pH values of the solution were adjusted by 0.1 M HCl or NaOH solutions. Adsorption experiments were performed in 10 mL centrifuge tube, and the adsorbent was swollen with deionized water before adsorption and dosage (weight of dry adsorbent) was 1 mg/mL. The centrifuge tubes were placed in an incubator shaker (QYC2112, Fuma, Shanghai, China) with desired temperature and fixed rotate speed of 160 rpm for 6 h. After adsorption processes, the adsorbent was separated by decantation and the supernatant was monitored on an atomic absorption spectrophotometer (Z-2000, Hitachi, Japan). For regeneration, the spent adsorbent was eluted with 1.0 M HCl solution and regenerated with 0.1 M NaOH solution, further washed with deionized water till neutral condition. Like the adsorption process, the elution and regeneration were performed in an incubator shaker for 2 h. Changes in adsorption amount were determined at every cycle. All the experiments were performed twice under identical condition where the relative errors were within 5%.

2.5. Simulated wastewater treatment

Single column and tandem two columns packed with Cellulose/PAM-3 were used to test the fixed-bed column adsorption performance. The adsorbent was swollen with deionized water and smashed into powder before filling the columns. The simulated wastewater was prepared by the Xiangjiang River water (Changsha, Hunan province, China) with addition of 50 mg/L Cd(II), Cu(II) and Pb(II), and pH value was adjusted to 5.00 ± 0.01. The influent was pumped up-flow through the column by a peristaltic pump. When the effluent concentration was higher than the Chinese industrial wastewater discharge limit, 0.1, 1.0 and 1.0 mg/L for Cd(II), Cu(II) and Pb(II), respectively, the single column and tandem two columns were regenerated and reused in the next cycle.

2.6. Industrial effluents treatment

The different dosages of Cellulose/PAM-3 and tandem two columns packed with Cellulose/PAM-3 were used to treat the practical industrial effluent from Minmetals Copper Industry located in Hengyang, Hunan province, China. The pH value of the wastewater was adjusted before the treatment. When the effluent concentration was higher than the Chinese industrial wastewater discharge limit, 0.1, 1.0, 1.0, 4.0 and 10.0 mg/L for Cd(II), Cu(II), Pb(II), Zn(II) and Fe(II), respectively, the columns were regenerated and reused in the next cycle.

3. Results and discussion

3.1. Characterization

The freeze-dried DNHs (Fig. S1) reveal a loose and macroporous network which is assembled by hybrid crosslinked sheet-like laminas cellulose and chemically crosslinked PAM. Benefit from the sheet-like laminar structures, the inside active sites of DNHs are more easily exposed. The swollen Cellulose/PAM DNHs have a supramolecular structure (Fig. S2b), containing a high moisture content ranges from 98% to 69% (Table S1). The large number of hydrophilic functional groups in the DNHs favors for water absorption, and it also is accessible to foreign molecules including heavy metal ions [25]. The XPS element analysis of Cellulose/PAM-1 (Table S2) shows that the carbon, oxygen, nitrogen and sodium in Cellulose/PAM-1 are 61.69%, 26.00%, 7.75% and 4.56%, respectively. The good mechanical property (Fig. S3a and Fig. S4) of the DNHs should be resulted from the synergy of two mechanisms: the cross-linking structure of cellulose network created via chemical and physical cross-linking strategy, and the highly interconnected DN structure [21]. The TGA curves (Fig. S3b) reveal that adsorbents are relatively stable below 200 °C. Fig. S3c shows the FTIR spectra of Cellulose/PAM DNHs, the intensity of each peak is roughly the same and confirms the coexistence of cellulose and PAM networks. The XRD pattern (Fig. S3d) also indicates the successful combination of cellulose and PAM. The ^{13}C CP/MAS spectrum (Fig. S5) of Cellulose/PAM-1 in a solid state indicates the coexistence of the cellulose and PAM networks in the Cellulose/PAM-1 and their mutual influence.

3.2. Effect of environmental conditions

Environmental conditions including pH and interfering ions may affect the surface charge of adsorbent and existing form of adsorbate, consequently influencing the ability of metal ions

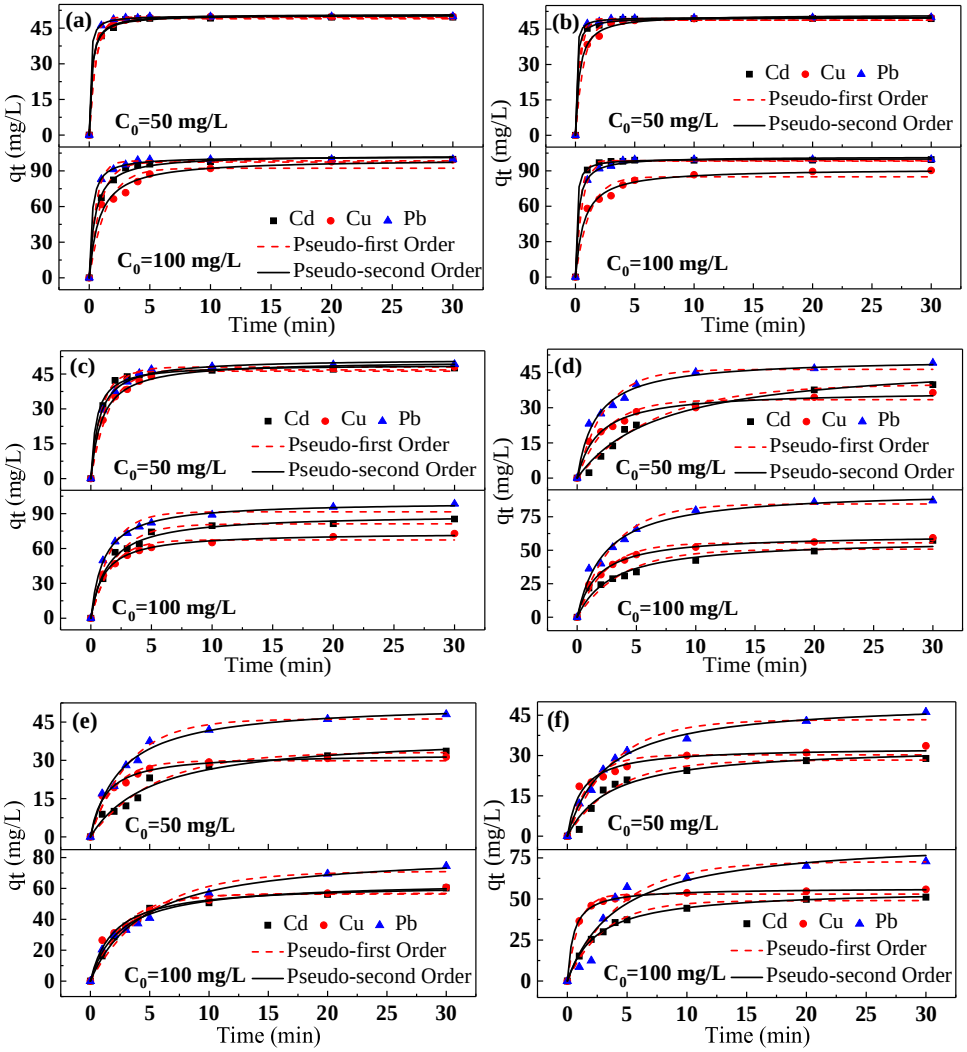

Fig. 2. Time-dependent adsorption of Cd(II)/Cu(II)/Pb(II) on (a) Cellulose/PAM-1, (b) Cellulose/PAM-2, (c) Cellulose/PAM-3, (d) Cellulose/PAM-4, (e) Cellulose/PAM-5, and (f) Cellulose/PAM-6, C_0 = 50/100 mg/L, T = 298 K, pH = 5.00 ± 0.01, m/V = 1 g/L.

removal. The uptake of heavy metal ions onto Cellulose/PAM DNHs is a pH-dependent process (Fig. S6). The adsorption efficiency increases quickly when pH value ranges from 2.00 to 3.00, then increases slowly at pH 3.00–4.00, and at last retains high sorption at pH above 5.00. The pH of bulk solution precipitation (pH_{BSP}) for Cd(II), Cu(II) and Pb(II) with initial concentration of 50 mg/L is 8.53, 5.86 and 5.87, respectively, and no precipitation occurred at pH below pH_{BSP}. Therefore, the excellent heavy metal removal at pH below pH_{BSP} is mainly attributed to adsorption rather than precipitation. The pH value at zero potential point (pH_{PZC}) of Cellulose/PAM DNHs is greater than 7.00 and increases with increasing amount of ECH (Fig. S6a and Table S1), due to the reduction of oxygen-containing functional groups. Generally, at pH<pH_{PZC}, the protonation reactions ($-O^- + H^+ \rightarrow -OH$) happen during the process, which is unfavorable for adsorption due to the electrostatic repulsion [26]. The Cellulose/PAM DNHs exhibit a relatively low adsorption efficiency at pH 2.00, which suggest that spent DNHs could be regenerated by acidic solutions.

In addition, the same positive-charge and high-level contents of the common cations may lead to surface adsorption sites competition toward heavy metal ions. Fig. S7 shows the effect of Na(I), K(I), NH_4(I), Ca(II) and Mg(II) on Cd(II)/Cu(II)/Pb(II) adsorption by Cellulose/PAM DNHs. For Cellulose/PAM-1 (Fig. S7a) and Cellulose/PAM-2 (Fig. S7b), the interfering ions had negligible effect on metal ions removal. Meanwhile, for the other four DNHs, the increasing concentrations of interfering ions had resulted in a decreased adsorption trend. Comparatively, the Pb(II) uptake behaviors slightly influenced by the presence of competing ions. Among these interfering ions, Ca(II) and Mg(II) have shown the greatest effect on the adsorption efficiency. This phenomenon can be explained by the following reasons: (i) With the decrease of active groups and increase of interfering ions, the competition for available sites is further strengthening [27]. (ii) Among these interfering ions, the ionic radius of Ca(II) and Mg(II) is relatively small, which will lead to stronger ions-active groups interaction [28]. (iii) The Cellulose/PAM DNHs sequester Cd(II)/Cu(II)/Pb(II) mainly through nonspecific electrostatic interactions [29].

3.3. Adsorption kinetics

Kinetic experiments were carried out by determining the solution Cd(II)/Cu(II)/Pb(II) contents at various time intervals. The adsorption amount of ions on the Cellulose/PAM-1, 2 and 3 increased rapidly in the first 5 min and equilibrium is achieved within 10 min, and the other three materials reached equilibrium at about 20 min (Fig. 2). As shown in Video S1, a small piece of Cellulose/PAM-3 was added into 3 g/L Cu(II) aqueous solution, and it quickly turns blue. The rapid kinetics are mainly attributed to

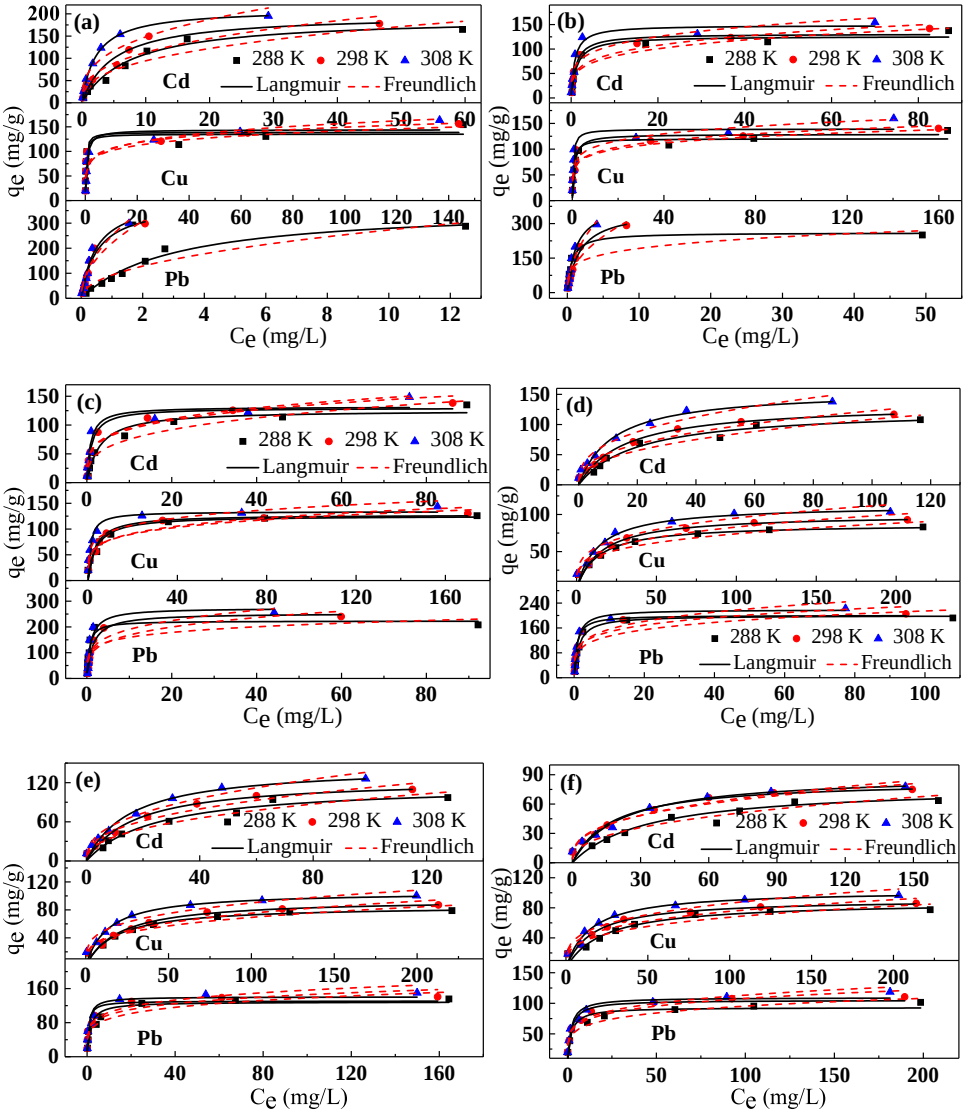

Fig. 3. Adsorption isotherms of Cd(II)/Cu(II)/Pb(II) on (a) Cellulose/PAM-1, (b) Cellulose/PAM-2, (c) Cellulose/PAM-3, (d) Cellulose/PAM-4, (e) Cellulose/PAM-5, and (f) Cellulose/PAM-6, $t_{contact}$ = 6 h, pH = 5.00 ± 0.01, m/V = 1 g/L.

the high permeability and sheet-like laminar structures, which favor for the diffusion and adsorption of metal ions. To describe the kinetic process, pseudo-first-order and pseudo-second-order models (see in SI) were employed to fit the kinetics data, and the kinetic parameters are summarized in Table S3-S8. The pseudo-second-order model gives the best fitting results according to the correlation coefficient (R^2). This result implies that the rate limiting step may be chemical sorption involving valency forces through the sharing of electrons exchange [30]. Furthermore, the intraparticle diffusion model (see in SI) was also used to describe the adsorption process (Fig. S8). Apparently, the curves contain two main steps and plots of the first step do not pass through the origin, indicating the multi-stages of adsorption and the first stage is not dominated by intraparticle diffusion process [31]. This can be attributed to the sheet-like laminar and macroporous structure of the DNHs.

Valuable information about the influencing factors of adsorption rate can be obtained through a comparative study of the as-prepared DNHs. The Cellulose/PAM-2 shows the largest pseudo-second-rate constant and advantage in adsorption rate. This can be attributed to the comprehensive effect of active sites amount and porous structure [32]. The Cellulose/PAM-1 shows smaller rate constant for the minimum pore size which resulted from the stack of cellulose sheet. Additionally, the K_d at equilibrium is shown in the following order: Cellulose/PAM–1 > 2 > 3 > 4 > 5, which is in positive correlation with active sites amount. Obviously, the adsorption ability of the as-prepared DNHs is directly dependent on active sites amount, while the adsorption rate not only depends on the functional groups content, but also the structure.

3.4. Adsorption modeling and thermodynamics

Temperature-dependent adsorption data fitted with Langmuir, Freundlich and Dubinin–Radushkevich (D-R) isotherm models (see in SI) are shown in Fig. 3 and Fig. S9. Adsorption amount increased with increasing initial heavy metal concentrations until reaching equilibrium. Noticeably, the residue concentration of Pb(II) remains 2.0 mg/L after using 1 g/L Cellulose/PAM-1 when the initial concentration is 300 mg/L. The nonlinear curve fitting parameters of Langmuir, Freundlich, Langmuir-Freundlich, RP and Temkin models are summarized in Table S9-S14. The adsorption isotherm data at 288, 298 and 308 K are better fitted with Langmuir adsorption model, which suggests that heavy metal adsorption onto

Cellulose/PAM DNHs is mostly via monolayer adsorption [33]. According to the fitting parameters, Cellulose/PAM-1 has the potential to remove Cd(II), Cu(II) and Pb(II) from aqueous solutions at 298 K with a maximum adsorption capacity of 198.48, 138.90 and 382.80 mg/g, respectively. Apparently, the maximum adsorption capacity decreases with increasing crosslinking dosage, and increases with increasing temperature. In addition, the R_L values are between 0 and 1 (Table S9-S14), which illustrate that the adsorption process is favourable [34]. The comparison of the maximum uptake of Cd(II)/Cu(II)/Pb(II) on cellulose based adsorbents is listed in Table S15. The adsorption capacity of Cellulose/PAM DNHs are comparatively high, revealing their great potential in dealing with heavy metal removal.

The thermodynamic parameters such as the standard free energy change (ΔG), standard enthalpy change (ΔH), and standard entropy changes (ΔS) were calculated according to the van't Hoff equation (see in SI) and average free energy (E) was calculated according to D-R isotherm equation. The negative values of ΔG and the positive values of ΔH and ΔS (Table S16) indicate that the adsorption of Cd(II), Cu(II) and Pb(II) on Cellulose/PAM DNHs are spontaneous and endothermic in nature, showing a high affinity [35]. The value of E (6.51–20.08 kJ/mol) (Table S17) is beyond the range of 8–16 kJ/mol, revealing that the adsorption process does not just occur with ion exchange [36].

3.5. Adsorption mechanism

In the above discussion, a preliminary conclusion can be inferred that this adsorption process does not just occur with ion exchange. To further understand the interaction mechanism, the FTIR, XRD and XPS studies were performed by choosing Pb(II) adsorption as a representative case. The DRS were performed by choosing Cu(II) adsorption as a representative case for the transition metal properties of Cu(II).

Fig. S10 shows the FTIR spectra of the Cellulose/PAM DNHs after adsorption of Pb(II). Compared to the spectra of Cellulose/PAM DNHs (Fig. S3c), the intensity of peaks corresponds to C—OH, C—O—C, and C—O stretching vibration weakened obviously, which indicates that cellulose network is involved in adsorption process. From the DRS (Fig. S11), there are obvious differences between Cellulose/PAM DNHs and Cellulose/PAM DNHs-Cu(II) (Cellulose/PAM-1 with adsorbed Cu(II)). After the adsorption of Cu(II), the d–d transition in metal center is seen by weak broad band in the range of 600–770 nm, suggesting that chemical interaction occurred between Cu(II) and Cellulose/PAM DNHs [37]. As can be seen from the XRD patterns of the Cellulose/PAM-1-Pb (Fig. S3d), the intensity of characteristic peaks ((110) and (200)) of cellulose II decrease and manifest as shoulder peaks compared to the Cellulose/PAM-1. The XRD patterns did not show any Pb phases so it is established that Pb is evenly dispersed in the adsorbent [38]. In the total XPS survey scans (Fig. S12a), new peaks of Pb(II) are observed in the Cellulose/PAM-1-Pb. As shown in Fig. S12b, the high-resolution scans for O 1 s in the Cellulose/PAM-1 can be grouped into three peaks at 535.8, 532.8, and 531.2 eV, corresponding to C—O—H, C—O—C, and C=O, respectively [39,40]. For Cellulose/PAM-1-Pb, slight shift is observed which reveal that oxygen-containing groups are involved in the adsorption process. In particular, after Pb(II) adsorption, the N 1 s peak remains unchanged (Fig. S12c), uncovering that nitrogen atom did not play a role in the adsorption process [41]. It is due to the lone pair of electrons of nitrogen atom in amide group were occupied, and the nitrogen atom was unlikely to donate the lone pairs to metal ions. Note that the Pb(II) binding energies for Cellulose/PAM-1-Pb are centered at 143.5 eV for Pb $4f_{5/2}$ and 138.6 eV for Pb $4f_{7/2}$ (Fig. S12d), respectively. Compared to the Pb(II) binding energies for purified $Pb(NO_3)_2$ (144.5 and 139.6 eV for Pb $4f_{5/2}$ and Pb $4f_{7/2}$, respectively) [29], a remarkable shift of 1.0 eV to lower binding energy of Pb 4f is observed. This shift indicates the formation of strong affinities between Pb(II) and Cellulose/PAM-1. Thus, the adsorption of ions by Cellulose/PAM DNHs is not a single process, mainly involved ion exchange and electrostatic attraction.

Table 1
The fixed-bed column parameters.

Parameter	Value	
	single column	two columns
Mass of dry sorbent (g)	4	8
Column diameter (mm)	14	14
Bed depth (mm)	150	150
Bed volume (BV) (mL)	23	46
Empty bed contact time (EBCT) (min)	5	8
Flow rate (mL/min)	4.06	5.75
Hydraulic loading rate (mm/min)	30	37.5

3.6. Selective adsorption

For the selective adsorption test, a mixed solution of Pb(II), Cu(II), Cd(II), Zn(II), Mn(II), Fe(II) and Ni(II) at pH 5.0 ± 0.01 was prepared, and initial concentration of all metal ions was set as 50 or 100 mg/L. As shown in Fig. S13, in the mixed solution, preferential adsorption of heavy metal ions depends on many factors, such as initial concentration, adsorbent species and dosages. The relative selectivity coefficients of Cellulose/PAM DNHs (Table S18-S23) for each specific metal ion are far greater than 1, suggesting its priority on the sorption of the corresponding ion and ability to remove other metal species in a mixed solution [42].

3.7. Sorption/desorption

The metal-loaded Cellulose/PAM DNHs were eluted by 1.0 M HCl solution, and then treated with 0.1 M NaOH solution, since the adsorption performance was highly dependent on the solution pH. Negligible discrepancy of adsorption amount is observed after 10 cycles of the adsorption-desorption process (Fig. S14). Moreover, the Cellulose/PAM DNHs can be separated directly from waste water through natural settling.

3.8. Simulated wastewater treatment

The laboratory small columns packed with adsorbent can be used to simulate the performance of pilot or full-scale systems [43]. The Xiangjiang River water was used to prepare the simulated wastewater (sampling site is shown in Fig. S15), the total carbon (TC), total organic carbon (TOC), inorganic carbon (IC), chemical oxygen demand (COD_{Cr}) and pH were 17.38, 1.54, 15.84, 8.0 mg/L and 7.24 (Table S24), respectively.

Simultaneous Cd(II)/Cu(II)/Pb(II) removal was achieved using fixed-bed columns packed with Cellulose/PAM-3, and the effluent concentrations were measured (Fig. 4). The column parameters are summarized in Table 1. For the single column, the treatment volumes reach 132 BV (3036 mL) for Cd(II), 168 BV (3864 mL) for Cu(II), and 264 BV (6072 mL) for Pb(II), the effluent concentrations are well below the Chinese industrial wastewater discharge limit. However, for the tandem two columns, the treatment volumes are 172.5 BV (7935 mL) for Cd(II), 195 BV (8970 mL) for Cu(II), and 292.5 BV (13455 mL) for Pb(II), respectively. Apparently, the adsorption saturation of the single column which requires regeneration is not achieved. Therefore, columns in series would be beneficial to take advantage of the adsorption potential of adsorbent. The mass balance calculation indicates that the total amount of Cd(II)/Cu(II)/Pb(II) loaded on the single column and tandem two

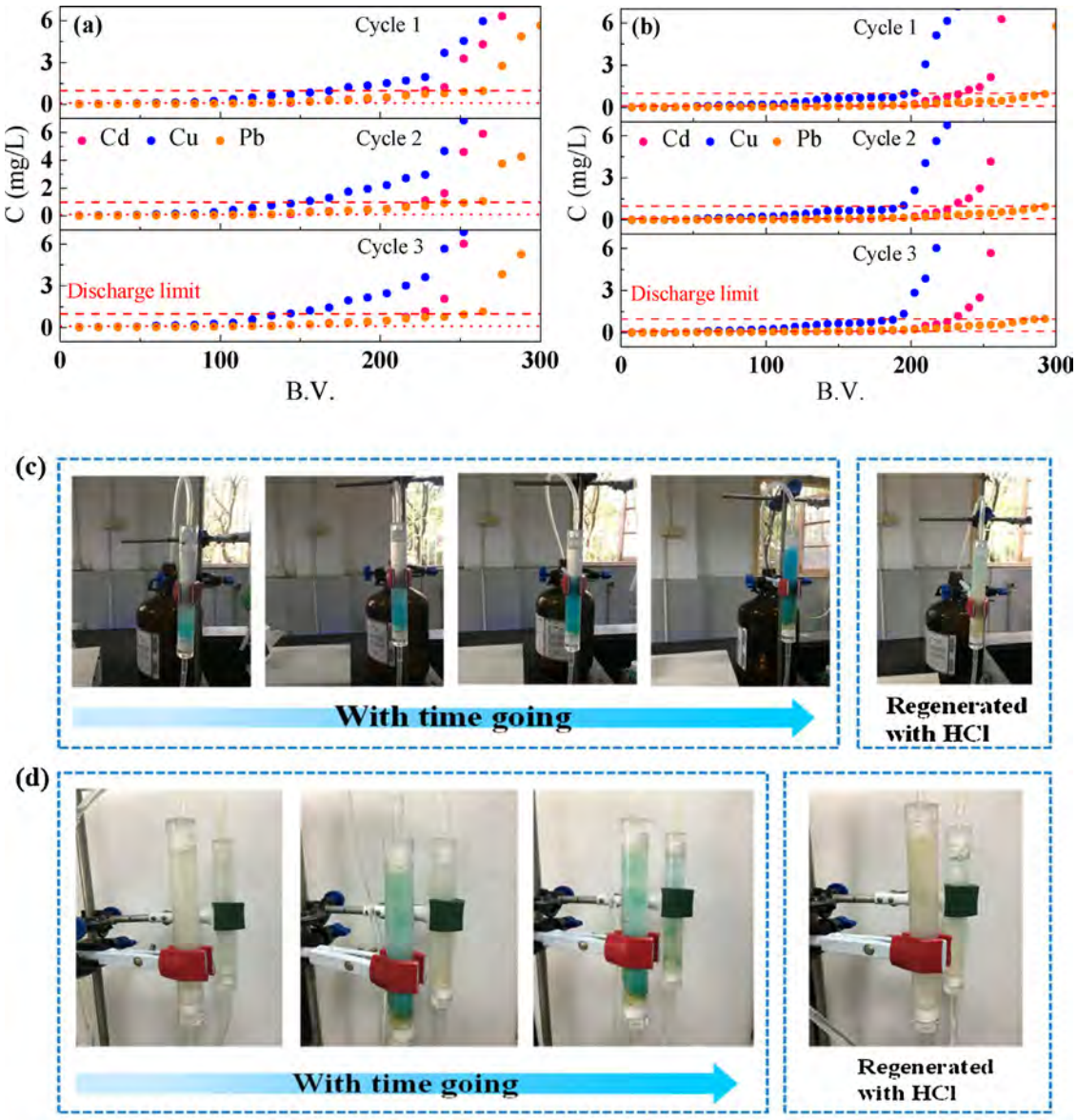

Fig. 4. Effluent Cd(II)/Cu(II)/Pb(II) concentrations from (a) single column, and (b) tandem two columns during three regeneration cycles as a function of bed volume, photographs of (c) single column, and (d) tandem two columns during adsorption process. pH = 5.00 ± 0.01, 1 BV is 23 and 46 mL for single column and two columns, respectively.

columns was 328.4/328.7/343.0 and 667.9/672.3/686.1 mg, respectively. The tandem two columns are efficient than single column because of the long mass transfer path, which facilitates more complete use of the adsorbent [44]. The cost analysis (see in SI) indicates that the amount of costs savings using columns in series increases as the process capacity increases. The adsorbed Cd(II)/Cu(II)/Pb(II) can be entirely eluted with approximately 2 BV (46 mL) and 2 BV (92 mL) of HCl solution for single column and tandem two columns (Fig. S16), respectively. Consequently, the metal ions were concentrated for the volume decreased from 6900 and 13800 mL to 46 and 92 mL for single column and tandem two columns, respectively. In addition, the other physicochemical characteristics values of the simulated wastewater that is treated with tandem two columns were reduced significantly (Table S24). Notably, the adsorption ability discrepancy is negligible after adsorption-desorption cycles, showing the excellent reusability of Cellulose/PAM-3.

3.9. Industrial effluent treatment

The physicochemical characteristics values (Table S24) of the industrial effluent (sampling site is shown in Fig. S17) were measured, and several kinds of main heavy metal ions existed such as Cd(II), Pb(II), Cu(II), Zn(II), and Fe with initial concentrations of 268.400, 7.600, 2324.700, 512.800, and 69.00 mg/L, respectively. The pH value of the raw wastewater was adjusted to 3.11, and different dosages of Cellulose/PAM-3 were used to remove heavy metal ions (Table 2). Obviously, the removal amount of all metal ions increased with increasing adsorbent dosage. With an adsorbent dosage of 6 g/L, the total concentration of residual metals is 0.54 mg/L and remaining concentration of each ion is lower than the discharge standard, and physicochemical characteristics values were also reduced significantly (Table S24).

Two columns packed with Cellulose/PAM-3 were applied to the industrial effluent treatment with a pH adjusted to 5.00, and effluent concentrations were measured (Fig. 5a). The treatment volumes

Table 2
Metal ions concentrations of industrial effluent before and after adsorption by different dosages of Cellulose/PAM-3.

Parameter		pH	Concentration (mg/L)				
			Cd	Cu	Pb	Fe	Zn
Dosage	0	0.98	268.400	2324.700	7.600	69.00	512.800
(g/L)	0	3.11	28.800	205.200	1.900	5.00	75.000
	1	3.11	17.250	168.950	0.070	4.00	51.670
	2	3.11	12.35	127.700	0.055	2.00	42.745
	3	3.11	4.550	80.900	0.005	1.60	26.800
	4	3.11	2.450	42.950	0.005	0.55	8.475
	5	3.11	0.340	2.590	0.005	0.10	0.350
	6	3.11	0.050	0.290	0.005	0.10	0.095
Removal rate		/	99.8%	99.8%	99.7%	98.0%	99.9%
Discharge limit		/	0.1	1.0	1.0	10.0	4.0

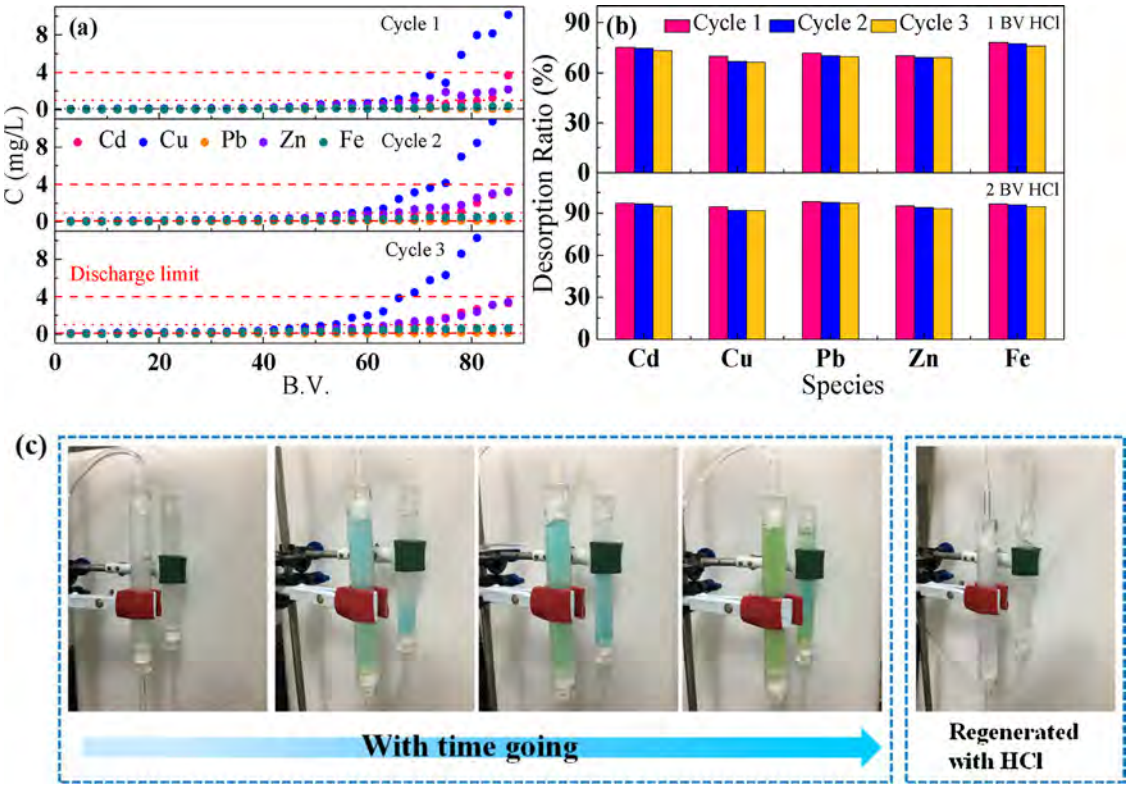

Fig. 5. (a) Effluent metal species concentrations from two columns during three regeneration cycles as a function of bed volume, (b) desorption ratio of metal species with different amount of 1.0 M HCl, and (c) photographs of the columns during adsorption process. pH = 5.00 ± 0.01, 1 BV is 46 mL.

reach 42 BV (1932 mL) for Cd(II), 63 BV (2898 mL) for Cu(II), 87 BV (4002 mL) for Pb(II), Zn(II) and Fe, respectively, and the effluent concentrations are well below the Chinese industrial wastewater discharge limit. Therefore, if the treatment volume is controlled below 42 BV (1932 mL), metal ions in the industrial effluent can be effectively removed. It takes only 420 min to process 42 BV (1932 mL) wastewater according to the bed contact time. Based on the mass balance calculation, when the treatment volume reaches 87 BV (4002 mL), the total amount of Cd(II)/Cu(II)/Pb(II)/Zn(II)/Fe loaded on the adsorbent is 111.5/723.2/10.6/289.6/17.0 mg. The desorption history of saturated columns reveals that metal ions loaded on the adsorbent can be entirely eluted with 2 BV (92 mL) 1.0 M HCl solution (Fig. 5b), and photographs are shown in Fig. 5c. Attractively, the treatment volumes retain respectively 36 BV (1656 mL) for Cd(II), 54 BV (2484 mL) for Cu(II), and 87 BV (4002 mL) for Pb(II), Zn(II) and Fe in the 3rd cycle. The discrepancy of treatment volumes in the 1 st and 3rd cycles should be attributed to the other impurities that occupies the adsorption sites. Overall, Cellulose/PAM DNHs show the potential of treating industrial effluent contains metal ions.

4. Conclusions

We have successfully prepared a series of DNHs based on cellulose derived from WCFs and explored the heavy metal adsorption performance of these materials. The three-dimensional porous structure and sheet-like laminar cellulose network offer promising contributions to heavy metal removal. The Cellulose/PAM DNHs exhibit fast kinetic, large adsorption capacities and reversible adsorption properties. The adsorption performance is highly dependent on the amount of cross linker (ECH) which is related to the number of active sites and adsorbent structure. In addition, fixed-bed columns packed with Cellulose/PAM-3 can effectively treat simulated wastewater and industrial effluent, and the regeneration of columns is operationally feasible. This study provides a novel route to recycle the WCFs, and at the same time it can be applied to the wastewater treatment, which is expected to guide

an effective way to recycle solid waste and produce low-cost adsorbent.

Acknowledgements

This work was supported by the National Natural Science Foundation of China (51378187, 51478171, 51672077); Hunan Provincial Natural Science Foundation of China (14JJ1015, 2017JJ2026).

Appendix A. Supplementary data

Supplementary data associated with this article can be found, in the online version, at https://doi.org/10.1016/j.jhazmat.2017.11.041.

References

[1] Y.D. Zou, X.X. Wang, A. Khan, P.Y. Wang, Y.H. Liu, A. Alsaedi, T. Hayat, X.K. Wang, Environmental remediation and application of nanoscale zero-valent iron and its composites for the removal of heavy metal ions: a review, Environ. Sci. Technol. 50 (2016) 7290–7304.
[2] F. Zhu, L.W. Li, J.D. Xing, Selective adsorption behavior of Cd(II) ion imprinted polymers synthesized by microwave-assisted inverse emulsion polymerization: adsorption performance and mechanism, J. Hazard. Mater. 321 (2017) 103–110.
[3] A. Macías-García, M. Gómez Corzo, M. Alfaro Domínguez, M. Alexandre Franco, J. Martínez Naharro, Study of the adsorption and electroadsorption process of Cu (II) ions within thermally and chemically modified activated carbon, J. Hazard. Mater. 328 (2017) 46–55.
[4] Z.L. Zhang, X.D. Zhang, D. Niu, Y.S. Li, J.L. Shi, Highly efficient and selective removal of trace lead from aqueous solutions by hollow mesoporous silica loaded with molecularly imprinted polymers, J. Hazard. Mater. 328 (2017) 160–169.
[5] I. Ali, New generation adsorbents for water treatment, Chem. Rev. 112 (2012) 5073–5091.
[6] E. Repo, J.K. Warchol, A. Bhatnagar, A. Mudhoo, M. Sillanpaa, Aminopolycarboxylic acid functionalized adsorbents for heavy metals removal from water, Water Res. 47 (2013) 4812–4832.
[7] Z. Tang, Y.F. Deng, T. Luo, Y.S. Xu, N.M. Zhu, Enhanced removal of Pb(II) by supported nanoscale Ni/Fe on hydrochar derived from biogas residues, Chem. Eng. J. 292 (2016) 224–232.
[8] H. Zhao, J.H. Xu, W.J. Lan, T. Wang, G.S. Luo, Microfluidic production of porous chitosan/silica hybrid microspheres and its Cu(II) adsorption performance, Chem. Eng. J. 229 (2013) 82–89.
[9] S.J. Xin, Z.Y. Zeng, X. Zhou, W.J. Luo, X.W. Shi, Q. Wang, H.B. Deng, Y.M. Du, Recyclable saccharomyces cerevisiae loaded nanofibrous mats with sandwich structure constructing via bio-electrospraying for heavy metal removal, J. Hazard. Mater. 324 (2017) 365–372.
[10] Z.Z. Guo, X.D. Zhang, Y. Kang, J. Zhang, Biomass-derived carbon sorbents for Cd(II) removal: activation and adsorption mechanism, ACS Sustainable Chem. Eng. 5 (2017) 4103–4109.
[11] S. Wagener, N. Dommershausen, H. Jungnickel, P. Laux, D. Mitrano, B. Nowack, G. Schneider, A. Luch, Textile functionalization and its effects on the release of silver nanoparticles into artificial sweat, Environ. Sci. Technol. 50 (2016) 5927–5934.
[12] D. Tian, X.X. Zhang, C.H. Lu, G.P. Yuan, W. Zhang, Z.H. Zhou, Solvent-free synthesis of carboxylate-functionalized cellulose from waste cotton fabrics for the removal of cationic dyes from aqueous solutions, Cellulose 21 (2013) 473–484.
[13] D.M. Alzate-Sánchez, B.J. Smith, A. Alsbaiee, J.P. Hinestroza, W.R. Dichtel, Cotton fabric functionalized with a β-cyclodextrin polymer captures organic pollutants from contaminated air and water, Chem. Mater. 28 (2016) 8340–8346.
[14] Z.H. Wang, Z.J. Yao, J.T. Zhou, Y. Zhang, Reuse of waste cotton cloth for the extraction of cellulose nanocrystals, Carbohydr. Polym. 157 (2017) 945–952.
[15] Y.H. Zhu, S. Yuan, D. Bao, Y.B. Yin, H.X. Zhong, X.B. Zhang, J.M. Yan, Q. Jiang, Decorating waste cloth via industrial wastewater for tube-type flexible and wearable sodium-ion batteries, Adv. Mater. 29 (2017) 1603719.
[16] J. Gong, H.J. Lin, J.W.C. Dunlop, J.Y. Yuan, Hierarchically arranged helical fiber actuators derived from commercial cloth, Adv. Mater. 29 (2017) 1605103.
[17] Y.Y. Han, X.X. Zhang, X.D. Wu, C.H. Lu, Flame retardant, heat insulating cellulose aerogels from waste cotton fabrics by in situ formation of magnesium hydroxide nanoparticles in cellulose gel nanostructures, ACS Sustainable Chem. Eng. 3 (2015) 1853–1859.
[18] H.S. Qi, Q.L. Yang, L.N. Zhang, T. Liebert, T. Heinze, The dissolution of cellulose in NaOH-based aqueous system by two-step process, Cellulose 18 (2010) 237–245.
[19] S. Hokkanen, A. Bhatnagar, M. Sillanpää, A review on modification methods to cellulose-based adsorbents to improve adsorption capacity, Water Res. 91 (2016) 156–173.
[20] R. Xu, G.Y. Zhou, Y.H. Tang, L. Chu, C.B. Liu, Z.B. Zeng, S.L. Luo, New double network hydrogel adsorbent: highly efficient removal of Cd (II) and Mn (II) ions in aqueous solution, Chem. Eng. J. 275 (2015) 179–188.
[21] H.Y. Jia, Z.J. Huang, Z.F. Fei, P.J. Dyson, Z. Zheng, X.L. Wang, Unconventional tough double-network hydrogels with rapid mechanical recovery self-healing, and self-gluing properties, ACS Appl. Mater. Interfaces 8 (2016) 31339–31347.
[22] J.L. Hou, X.Y. Ren, S. Guan, L.J. Duan, G.H. Gao, Y. Kuai, H.X. Zhang, Rapidly recoverable anti-fatigue, super tough double network hydrogels reinforced by macromolecular microspheres, Soft Matter 13 (2017) 1357–1363.
[23] Q. Chen, L. Zhu, C. Zhao, Q.M. Wang, J. Zheng, A robust, one-pot synthesis of highly mechanical and recoverable double network hydrogels using thermoreversible sol-gel polysaccharide, Adv. Mater. 25 (2013) 4171–4176.
[24] L. Chu, C.B. Liu, G.Y. Zhou, R. Xu, Y.H. Tang, Z.B. Zeng, S.L. Luo, A double network gel as low cost and easy recycle adsorbent: highly efficient removal of Cd(II) and Pb(II) pollutants from wastewater, J. Hazard. Mater. 300 (2015) 153–160.
[25] Z.X. Xue, S.T. Wang, L. Lin, L. Chen, M.J. Liu, L. Feng, L. Jiang, A novel superhydrophilic and underwater superoleophobic hydrogel-coated mesh for oil/water separation, Adv. Mater. 23 (2011) 4270–4273.
[26] G.Y. Zhou, C.B. Liu, Y.H. Tang, S.L. Luo, Z.B. Zeng, Y.T. Liu, R. Xu, L. Chu, Sponge-like polysiloxane-graphene oxide gel as a highly efficient and renewable adsorbent for lead and cadmium metals removal from wastewater, Chem. Eng. J. 280 (2015) 275–282.
[27] J.H. Ma, G.Y. Zhou, L. Chu, Y.T. Liu, C.B. Liu, S.L. Luo, Y.F. Wei, Efficient removal of heavy metal ions with an EDTA functionalized chitosan/polyacrylamide double network hydrogel, ACS Sustainable Chem. Eng. 5 (2017) 843–851.
[28] T. Wang, W. Liu, L. Xiong, N. Xu, J.R. Ni, Influence of pH ionic strength and humic acid on competitive adsorption of Pb(II), Cd(II) and Cr(III) onto titanate nanotubes, Chem. Eng. J. 215-216 (2013) 366–374.
[29] Q.M. Peng, J.X. Guo, Q.R. Zhang, J.Y. Xiang, B.Z. Liu, A.G. Zhou, R.P. Liu, Y.J. Tian, Unique lead adsorption behavior of activated hydroxyl group in two-dimensional titanium carbide, J. Am. Chem. Soc. 136 (2014) 4113–4116.
[30] Y.X. Song, T.T. Qiang, M. Ye, Q.Y. Ma, Z. Fang, Metal organic framework derived magnetically separable 3-dimensional hierarchical Ni@C nanocomposites: synthesis and adsorption properties, Appl. Surf. Sci. 359 (2015) 834–840.
[31] Z. Zarghami, A. Akbari, A.M. Latifi, M.A. Amani, Design of a new integrated chitosan-PAMAM dendrimer biosorbent for heavy metals removing and study of its adsorption kinetics and thermodynamics, Bioresour. Technol. 205 (2016) 230–238.
[32] W. Zhang, X.H. He, G. Ye, R. Yi, J. Chen, Americium(III) capture using phosphonic acid-functionalized silicas with different mesoporous morphologies: adsorption behavior study and mechanism investigation by EXAFS/XPS, Environ. Sci. Technol. 48 (2014) 6874–6881.
[33] Y.F. Zhu, Y.A. Zheng, F. Wang, A.Q. Wang, Monolithic supermacroporous hydrogel prepared from high internal phase emulsions (HIPEs) for fast removal of Cu^{2+} and Pb^{2+}, Chem. Eng. J. 284 (2016) 422–430.
[34] K.Y. Foo, B.H. Hameed, Insights into the modeling of adsorption isotherm systems, Chem. Eng. J. 156 (2010) 2–10.
[35] Z.C. Sun, Y.G. Liu, Y.Q. Huang, X.F. Tan, G.M. Zeng, X.J. Hu, Z.Z. Yang, Fast adsorption of Cd^{2+} and Pb^{2+} by EGTA dianhydride (EGTAD) modified ramie fiber, J. Colloid Interface Sci. 434 (2014) 152–158.
[36] A. Günay, E. Arslankaya, I. Tosun, Lead removal from aqueous solution by natural and pretreated clinoptilolite: adsorption equilibrium and kinetics, J. Hazard. Mater. 146 (2007) 362–371.
[37] M. Zendehdel, F. Zamani, MCM-41-supported NNO type Schiff base complexes: a highly selective heterogeneous nanocatalyst for esterification, Diels?Alder and aldol condensation, J. Porous Mater. 24 (2017) 1263–1277.
[38] H.X. Qi, S.R. Zhai, Z.Z. Wang, B. Zhai, Q.D. An, Designing recyclable Cu/ZrSBA-15 for efficient thiophene removal, Microporous Mesoporous Mat. 217 (2015) 21–29.
[39] J.H. Zhou, Z.J. Sui, J. Zhu, P. Li, D. Chen, Y.C. Dai, W.K. Yuan, Characterization of surface oxygen complexes on carbon nanofibers by TPD, XPS and FT-IR, Carbon 45 (2007) 785–796.
[40] J. Huang, M. Ye, Y.Q. Qu, L.F. Chu, R. Chen, Q.Z. He, D.F. Xu, Pb (II) removal from aqueous media by EDTA-modified mesoporous silica SBA-15, J. Colloid Interface Sci. 385 (2012) 137–146.
[41] G.Y. Zhou, C.B. Liu, L. Chu, Y.H. Tang, S.L. Luo, Rapid and efficient treatment of wastewater with high-concentration heavy metals using a new type of hydrogel-based adsorption process, Bioresour. Technol. 219 (2016) 451–457.
[42] J.J. Wang, Z.K. Li, Enhanced selective removal of Cu(II) from aqueous solution by novel polyethylenimine-functionalized ion imprinted hydrogel: behaviors and mechanisms, J. Hazard. Mater. 300 (2015) 18–28.
[43] M. Kanematsu, T.M. Young, K. Fukushi, P.G. Green, J.L. Darby, Individual and combined effects of water quality and empty bed contact time on As(V) removal by a fixed-bed iron oxide adsorber: implication for silicate precoating, Water Res. 46 (2012) 5061–5070.
[44] L. Yan, Y.Y. Huang, J.L. Cui, C.Y. Jing, Simultaneous As(III) and Cd removal from copper smelting wastewater using granular TiO_2 columns, Water Res. 68 (2015) 572–579.